MOF–Polymer Composites Hot Paper

Deutsche Ausgabe: DOI: 10.1002/ange.201606926
Internationale Ausgabe: DOI: 10.1002/anie.201606926

MOF-5-Polystyrene: Direct Production from Monomer, Improved Hydrolytic Stability, and Unique Guest Adsorption

*Nipuni-Dhanesha H. Gamage, Kyle A. McDonald, and Adam J. Matzger**

Abstract: *An unprecedented mode of reactivity of Zn_4O-based metal–organic frameworks (MOFs) offers a straightforward and powerful approach to polymer-hybridized porous solids. The concept is illustrated with the production of MOF-5-polystyrene wherein polystyrene is grafted and uniformly distributed throughout MOF-5 crystals after heating in pure styrene for 4–24 h. The surface area and polystyrene content of the material can be fine-tuned by controlling the duration of heating styrene in the presence of MOF-5. Polystyrene grafting significantly alters the physical and chemical properties of pristine MOF-5, which is evident from the unique guest adsorption properties (solvatochromic dye uptake and improved CO_2 capacity) as well as the dramatically improved hydrolytic stability of composite. Based on the fact that MOF-5 is the best studied member of the structure class, and has been produced at scale by industry, these findings can be directly leveraged for a range of current applications.*

Metal–organic frameworks (MOFs) hybridized with organic polymers are an emerging class of composite materials with potential to combine properties sought after in industrial separation processes.[1] MOFs are useful to gain defined porosities with high surface areas, crystallinity, regularity, topological diversity, and ability to tune functionality.[2] However, these crystalline materials have poor mechanical properties and are challenging to process.[3] Organic polymers have the potential to impart hydrolytic stability, processability, and compatibility with organic phases to MOFs. Thus, such MOF–polymer composites, including membranes, are of interest for a wide variety of adsorption and separation applications.[4]

For optimal performance of MOF–polymer composite membranes, a high compatibility between the MOF and the organic polymer phase is important. The common methods of incorporating MOFs into polymer matrices suffer from poor MOF–polymer adhesion, interfacial voids, and MOF particle aggregation.[5] Several synthetic attempts have been made to modify the surface of the MOFs and/or polymers to covalently link them for enhancing the compatibility between the polymer matrices and MOFs.[6] Previously, we successfully performed surface modification of MOFs for covalent polymer attachment and also retained a high surface area (2289–2857 $m^2 g^{-1}$) in the polymer-MOF composite by adopting a core–shell architecture.[7] In addition to being somewhat laborious, the core–shell approach dictates that only kinetic selectivities can be obtained in a separation process because the bulk of the material is unfunctionalized. Imperfections in the polymer shell compromise even this kinetic selectivity, and in practice, only marginal gains in hydrolytic stability were observed in spite of using hydrophobic polymers and such results are inferior to simple silicone polymer coatings or polymer-grafted linkers.[2a,4b,6b,8]

Herein, we report the synthesis of a MOF-5-PS composite material with a uniform distribution of strongly bound polystyrene, formed by a simple, initiator-free synthesis. The MOF-5-PS composite is formed by heating neat styrene in the presence of MOF-5 at 65 °C. The material produced after 24 h of heating (MOF-5-PS-24h) gains remarkable hydrolytic stability over pristine MOF-5. Dye and CO_2 gas adsorption properties of this composite demonstrate that polystyrene grafting significantly alters the physical and chemical properties of pristine MOF-5.

An appreciable content of polystyrene was grafted onto MOF-5 crystals by heating in neat pure styrene for at least 4 h at 65 °C. Styrene was heated for 4, 5, 8, 16, and 24 h at 65 °C in the presence of MOF-5 to obtain the composites MOF-5-PS-4h to MOF-5-PS-24h with increasing polymer contents (Scheme 1, See Supporting Information, Section I for experimental details). The maintenance of correct temperature is essential for the reproducibility of results. This strongly bound polystyrene is retained in the MOF-5-PS composites even after heating at 60 °C in THF. Physisorbed high molecular weight polystyrene is removed under such conditions from the MOF-5 crystals based on our control experiments (Supporting Information, Section I).

[*] Dr. N.-D. H. Gamage, K. A. McDonald, Prof. A. J. Matzger
University of Michigan
Department of Chemistry
930 N. University Ave, Ann Arbor, MI 48109 (USA)
E-mail: matzger@umich.edu
Prof. A. J. Matzger
Department of Macromolecular Science and Engineering, University of Michigan
Ann Arbor, MI 48109 (USA)
Supporting information and the ORCID identification number(s) for the author(s) of this article can be found under http://dx.doi.org/10.1002/anie.201606926.

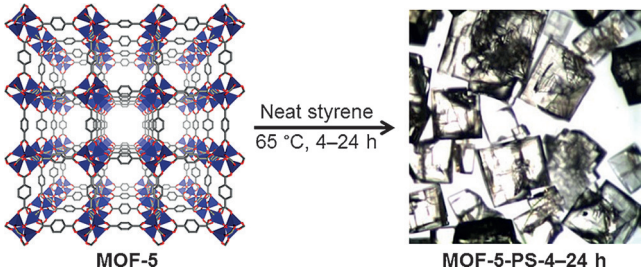

Scheme 1. Synthetic scheme for direct production of MOF-5-PS-4–24h composites from monomer.

Polymerization of styrene in the presence of MOF-5 at 65 °C up to 24 h does not alter the crystallinity of MOF-5 according to powder X-ray diffraction (PXRD; Supporting Information, Figure S1). The weight percentages of polystyrene in the MOF-5-PS composites were investigated using thermogravimetric analysis (TGA) to observe mass loss corresponding to depolymerization of polystyrene. The TGA curves of MOF-5-PS-4–24h samples and as synthesized MOF-5 are shown in Figure 1. The depolymerization of polymer is well separated from MOF decomposition enabling facile quantification of loading (Supporting Information, Figure S2–4).

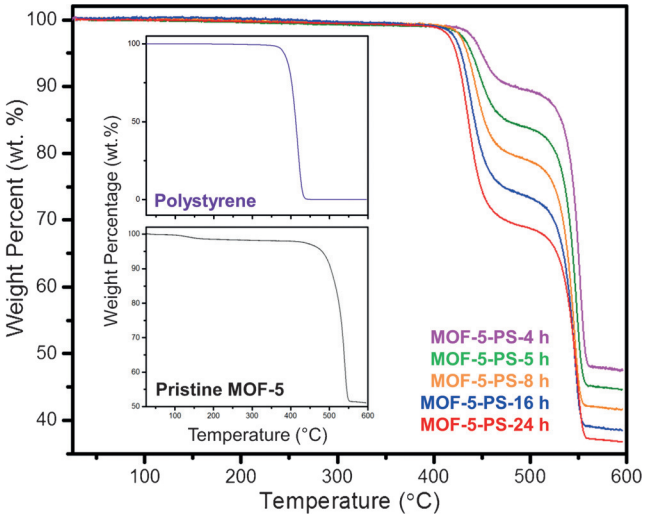

Figure 1. TGA curves of MOF-5-PS-4–24h, polystyrene, and pristine MOF-5.

The weight percentage of polystyrene in the composite crystals increases with increased duration of heating in styrene (Figure 1). There is approximately 9.4–30.1 wt% polystyrene grafted in the MOF-5-PS composite after 4–24 h of polymerization at 65 °C (Table 1). Thus, the weight percentage of polystyrene in MOF-5-PS composites can be tuned by changing the duration of heating styrene in the presence of MOF-5.

N_2 sorption isotherms of the MOF-5-PS composites after 4, 5, 8, 16, and 24 h of polymerization of styrene are shown in Figure 2. The corresponding surface areas obtained by applying the BET approximation[9] to the data obtained

Table 1: Weight percentages of polystyrene and BET surface areas of MOF-5-PS-4–24h.

Polymerization time [h]	TGA weight percentage of polystyrene [%]	BET surface area [m^2 g]
0	–	3509
4	9.4	2780
5	15.1	2496
8	20.0	2163
16	25.3	1868
24	30.1	1611

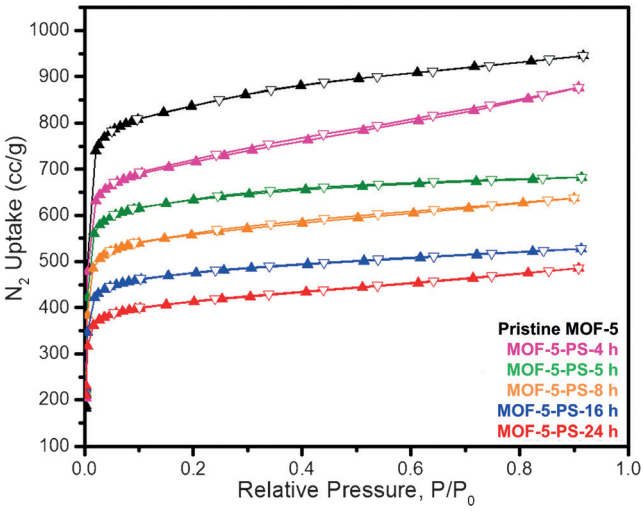

Figure 2. N_2 sorption isotherms of pristine MOF-5 and MOF-5-PS-4–24h composites (Adsorption data are shown in full symbols while desorption data are shown in hollow symbols).

from N_2 sorption experiments are shown in Table 1. Increasing the duration of heating styrene in the presence of MOF-5 leads to more polystyrene grafting and thus, reduction of surface area. The surface areas of MOF-5-PS composites are in the range of 2780–1611 $m^2 g^{-1}$ after 4–24 h of polymerization of styrene at 65 °C. As the percentage of MOF-5 in the composite decreases there is a linear decrease of BET surface area (Correlation graphs of the surface areas obtained for the MOF-5-PS composites to the duration of heating and the percentage of MOF-5 are shown in Supporting Information, Figure S5).

Complete digestion of the MOF-5-PS composites in 1 M NaOH was not possible due to high hydrophobicity. However, after basic treatment, it was possible to dissolve polymer in THF to allow characterization of the polymer molecular weight and molecular weight distribution by gel permeation chromatography (GPC). After 24 h of polymerization of styrene in the presence of MOF-5 at 65 °C, a high molecular weight polymer of 577 kDa (M_n) was extracted from the digested MOF-5-PS composite with a dispersity ($Đ$) of 1.31 (Supporting Information, Figure S6). Similar high molecular weight polymers with approximately similar dispersities were observed by GPC from the MOF-5-PS samples after 4, 5, 8, and 16 h of polymerization of styrene at 65 °C (Supporting Information, Table S1).

The high molecular weight of polystyrene precludes polymer isolation within a single pore of MOF-5. Indeed, approximation using the bulk density of polystyrene indicates that a chain of no more than twelve repeat units could fit in a single MOF-5 pore with a diameter of 12.5 Å. If stretched to a totally linear conformation, an oligomer of only five repeat units could sit inside a pore. At the molecular weight of 577 kDa, a polystyrene chain has a diameter of 12 nm and has a volume equivalent to approximately 500 MOF-5 pores (Supporting Information, Section VI). In contrast, if stretched to a totally linear conformation, this polystyrene would occupy approximately 1100 pores of MOF-5 (Supporting

Information, Section VI). As shown below, the behavior of the polymer lies between these extremes.

The presence of polystyrene in the MOF-5-PS composites was confirmed by Raman microspectroscopy. In addition to characteristic signals of MOF-5,[10] Raman peaks at 1001 and 1030 cm^{-1} corresponding to the breathing mode of the aromatic carbon ring and bending modes of C–H bonds of polystyrene, respectively, were present (Supporting Information, Figures S7 and S8). A Raman mapping experiment was performed on a sectioned MOF-5-PS-24h crystal embedded in epoxy resin to study the distribution of polystyrene by examining the distribution of the 1001 cm^{-1} peak. According to the Raman mapping image and the white-light image (Figure 3 A,B) polystyrene is uniformly distributed throughout the MOF-5 crystal.

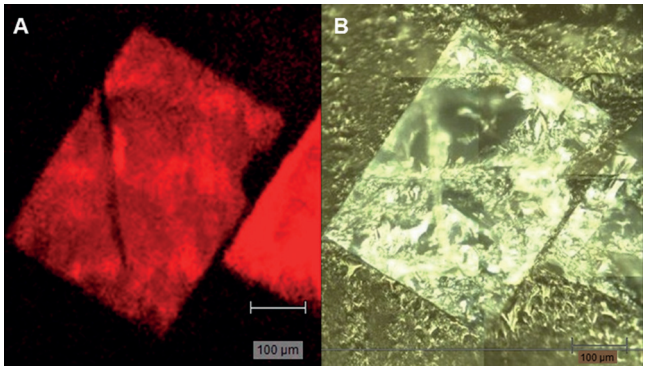

Figure 3. Raman mapping data of MOF-5-PS-24h: A) Raman map of area for the 1001 cm^{-1} peak, shown in red, of the cross-sectioned MOF-5-PS embedded in epoxy resin; B) A white-light image of the cross-sectioned MOF-5–PS embedded in epoxy resin showing two distinct crystals.

Though the micron scale uniformity of polystyrene distribution is clearly shown by Raman mapping, what is occurring on the level of the pores is not observable directly. Therefore, the pore size distributions of MOF-5-PS composites were obtained by applying the non-local density functional theory (NLDFT)[11] with the cylindrical pore model and using the DFT and Monte Carlo approximation to the data obtained from Ar sorption experiments. A pore size distribution plot of the MOF-5-PS-24h composite is shown for comparison with the pore size distribution of pristine MOF-5 in Figure 4. Pore size distribution plots for MOF-5-PS-4–16 h composites are provided in Supporting Information, Figures S9 and S10. Pristine MOF-5 mostly contains pore widths of approximately 12.5 Å. After grafting polystyrene using the polymerization process for 24 h there is a decrease in the content of pores of 12.5 Å and the major pore width obtained is approximately 11.5 Å. Smaller pore widths in the range of 5.2–9.6 Å that are absent in pristine MOF-5 were observed for the MOF-5-PS composites. The pore size distribution of MOF-5-PS composites shifts towards the range of 5.2–11.5 Å when the duration of heating styrene is increased (Supporting Information, Figures S9 and S10). Taken together with the Raman mapping data, this indicates that as the polymer loading increases, polystyrene is distributed throughout the

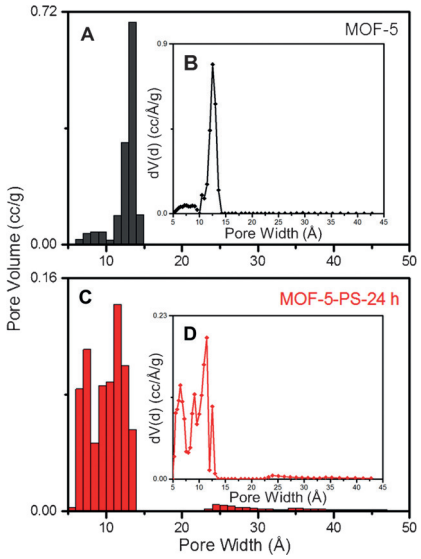

Figure 4. Pore volume histograms and differential pore volume distribution plots of pristine MOF-5 (A and B) and MOF-5-PS-24h (C and D).

available pore space and unoccupied pores are very rare. Thus, the MOF-5-PS composite material obtained via this simple synthetic method alters the material sufficiently that the composites may show unique sorption properties in which the thermodynamics of adsorption are altered rather than only the kinetics.

The hydrolytic stability of the MOF-5-PS-24h and pristine MOF-5 were studied after keeping the corresponding crystals at 53 % relative humidity (RH). Based on the PXRD patterns, pristine MOF-5 degraded within 4 h whereas the MOF-5-PS composite was stable for over 3 months (Supporting Information, Figures S11 and S12). This is consistent with previous reports for degradation rates of MOF-5.[12] The surface area obtained by applying the BET approximation to the data obtained from N_2 sorption of the MOF-5-PS composite after 3 months under 53 % RH was 1556 $m^2 g^{-1}$, which indicates that there is no significant reduction in the porosity of the composite (Supporting Information, Figure S13). Thus, a dramatic improvement in hydrolytic stability was achieved with this novel MOF-5-PS composite and this argues strongly for the drastic change in the chemical environment within the pores.

To probe changes in polarity of the pore environment of MOF-5-PS-24h composite versus pristine MOF-5, dye adsorption studies were performed. Solvatochromic behavior between a dye adsorbed in MOF-5-PS-24h and pristine MOF-5 can be employed to determine changes in surface polarity. Chosen dyes were methyl red and Nile red because of their ability to diffuse into constricted pores. The microscopic images of methyl red and Nile red adsorbed to MOF-5-PS-24h and MOF-5 crystals and the solid state UV/Vis spectra are shown in Figure 5. Based on the solid-state UV/Vis spectra, both methyl red and Nile red adsorbed in MOF-5-PS-24h show blue-shifted centroids of the peak envelopes with respect to the dyes adsorbed on pristine MOF-5. In both cases this is consistent with a less-polar environment in the pores

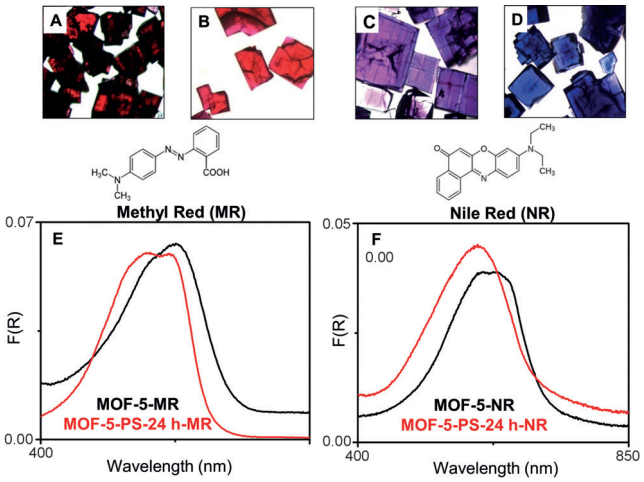

Figure 5. Microscopic images of methyl red and Nile red adsorbed MOF-5-PS-24h and MOF-5 crystals: A) methyl red dye adsorbed MOF-5-PS-24h; B) methyl red dye adsorbed MOF-5; C) Nile red dye adsorbed MOF-5-PS-24h; D) Nile red dye adsorbed MOF-5. Solid-state UV/Vis spectra: E) methyl red adsorbed MOF-5-PS-24h and MOF-5; F) Nile red adsorbed MOF-5-PS-24h and MOF-5.

upon incorporation of polymer. This conclusion is based on previous studies of solvent polarity effects on the absorption maxima for methyl red and Nile red.[13] Hence, the chemical and physical properties of MOF-5 has significantly changed with the uniform distribution of polystyrene in the MOF-5-PS-24h composite.

Variations in the pore environment of MOF-5-PS-4, 8, and -24h composites versus pristine MOF-5 were further analyzed by CO_2 adsorption studies (Supporting Information, Table S3 and Figure S14). The CO_2 adsorption isotherms obtained at 1 atm and 298 and 273 K are shown in Figure 6. Impressively, the CO_2 adsorption capacities of the MOF-5-PS composites are greater than pristine MOF-5 at both temperatures in spite of the lower surface areas. The maximum adsorption capacity was observed for the MOF-5-PS-8h composite at both 298 and 273 K. The higher CO_2 adsorption capacities can be attributed to the change of the pore environment with partial pore filling[14] by polystyrene and the optimum pore filling was obtained for the MOF-5-PS-8h composite. Thus, the pore

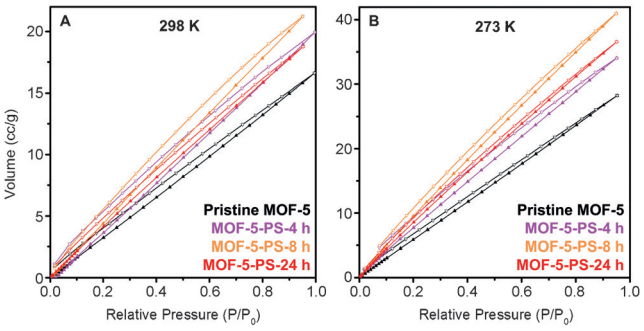

Figure 6. CO_2 adsorption isotherms of MOF-5-PS-4, -8, and -24h and pristine MOF-5 obtained at 1 atm: A) 298 K and B) 273 K (Adsorption data are shown in full symbols while desorption data are shown in open symbols).

environment is significantly altered in the MOF-5-PS composites with respect to pristine MOF-5.

Although a mechanistic understanding of the origin of grafting in MOF-5-PS has yet to be achieved, some observations are worth noting. Methyl methacrylate (MMA) does not form a grafted polymer with MOF-5 at 65 °C and thus, requires initiator grafting.[7] Styrene is different than MMA in several key aspects. Pure styrene is known to undergo self-initiated thermal polymerization at a rate of 0.1 % per hour at 60 °C in the absence of initiators.[15] Styrene is one of the few monomers known to undergo self-initiated thermal polymerization in the absence of impurities. According to the proposed Mayo mechanism,[15a] the self-initiated thermal polymerization of styrene is an initiator-free radical based process. There have been reports of experimental evidence[15b,16] as well as theoretical studies[15d] for the occurrence of the Mayo mechanism. High molecular weight polymers with similar dispersities were observed when neat styrene was polymerized in the presence of MOF-5 for varying durations or in the absence of MOF-5. Styrene is also prone to cationic polymerization and the potential role of cationic initiation merits investigations. Mechanistic investigations of the styrene polymerization process and grafting of polystyrene are underway and initial findings of inhibition of polymer grafting with the addition of BHT at approximately 250 ppm is consistent with a radical path.

The synthetic method described herein can be used with other MOFs including IRMOF-3, MOF-177, and HKUST-1. Also, functionalized styrene monomers, such as 4-bromo styrene can be used to obtain polymer grafted MOF-5-PS composites. Thus, this method can be employed to obtain versatile MOF and polymer composites with various chemical and physical properties.

In conclusion, we have obtained a novel MOF-5-PS composite material through a simple synthetic method avoiding laborious synthetic modifications and polymerization initiators. The MOF-5-PS-24 h composite is much greater in hydrolytic stability (over 3 months) with respect to pristine MOF-5 (4 h) at the relative humidity of 53 %. The solvatochromic behavior of methyl red and Nile red dyes adsorbed on MOF-5-PS-24h versus pristine MOF-5 demonstrates that the pore environment of MOF-5 is significantly changed after the polymer grafting. The MOF-5-PS composites also have higher CO_2 adsorption capacities at 1 atm and 298 and 273 K with respect to pristine MOF-5, a result of the significantly altered pore environment. Realizing such dramatic changes in properties after grafting polystyrene onto MOFs with this simple method allows versatile metal–organic framework and polymer composite materials for a wide variety of adsorption and separation applications.

Acknowledgements

This work was supported by the Department of Energy (Award # DE-SC0004888). K.A.M. gratefully acknowledges support from the National Science Foundation Graduate Research Fellowship Program (NSF-GRFP). We would also like to thank Derek S. Frank for his assistance in calculating

the theoretical distribution of polystyrene in MOF-5 and Dr. Antek Wong-Foy for his assistance in the gas sorption experiments.

Keywords: adsorption · hydrolytic stability · metal–organic frameworks · MOF–polymer composites · polymers

How to cite: *Angew. Chem. Int. Ed.* **2016**, *55*, 12099–12103
Angew. Chem. **2016**, *128*, 12278–12282

[1] a) H. Zhu, Q. Zhang, S. Zhu, *ACS Appl. Mater. Interfaces* **2016**, 8, 17395–17401; b) C. Le Calvez, M. Zouboulaki, C. Petit, L. Peeva, N. Shirshova, *RSC Adv.* **2016**, *6*, 17314–17317; c) P. Su, W. Li, C. Zhang, Q. Meng, C. Shen, G. Zhang, *J. Mater. Chem. A* **2015**, *3*, 20345–20351; d) Y. Zhang, X. Feng, H. Li, Y. Chen, J. Zhao, S. Wang, L. Wang, B. Wang, *Angew. Chem. Int. Ed.* **2015**, *54*, 4259–4263; *Angew. Chem.* **2015**, *127*, 4333–4337; e) H. Liu, H. Zhu, S. Zhu, *Macromol. Mater. Eng.* **2015**, *300*, 191–197; f) I. Erucara, S. Keskin, *J. Membr. Sci.* **2012**, *407–408*, 221–230; g) L. Bromberg, X. Su, T. A. Hatton, *Chem. Mater.* **2014**, *26*, 6257–6264; h) R. Zhang, S. Ji, N. Wang, L. Wang, G. Zhang, J.-R. Li, *Angew. Chem. Int. Ed.* **2014**, *53*, 9775–9779; *Angew. Chem.* **2014**, *126*, 9933–9937; i) X. Liang, F. Zhang, W. Feng, X. Zou, C. Zhao, H. Na, C. Liu, F. Sun, G. Zhu, *Chem. Sci.* **2013**, *4*, 983–992; j) J. Huo, M. Marcello, A. Garai, D. Bradshaw, *Adv. Mater.* **2013**, *25*, 2717–2722; k) H. J. Lee, W. Cho, M. Oh, *Chem. Commun.* **2012**, *48*, 221–223; l) D. Zhao, S. Tan, D. Yuan, W. Lu, Y. H. Rezenom, H. Jiang, L.-Q. Wang, H.-C. Zhou, *Adv. Mater.* **2011**, *23*, 90–93; m) L. D. O'Neill, H. Zhang, D. Bradshaw, *J. Mater. Chem.* **2010**, *20*, 5720–5726.

[2] a) Z. Zhang, H. T. H. Nguyen, S. A. Miller, S. M. Cohen, *Angew. Chem. Int. Ed.* **2015**, *54*, 6152–6157; *Angew. Chem.* **2015**, *127*, 6250–6255; b) S. L. James, *Chem. Soc. Rev.* **2003**, *32*, 276–288; c) M. Eddaoudi, J. Kim, N. Rosi, D. Vodak, J. Wachter, M. O'Keeffe, O. M. Yaghi, *Science* **2002**, *295*, 469–472; d) T.-H. Park, K. Koh, A. G. Wong-Foy, A. J. Matzger, *Cryst. Growth Des.* **2011**, *11*, 2059–2063; e) A. Dutta, A. G. Wong-Foy, A. J. Matzger, *Chem. Sci.* **2014**, *5*, 3729–3734; f) W. R. Wade, T. Corrales-Sanchez, T. C. Narayan, M. Dincă, *Energy Environ. Sci.* **2013**, *6*, 2172–2177; g) K. Biradha, M. Fujita, *Chem. Commun.* **2001**, 15–16.

[3] a) G. Dong, H. Li, V. Chen, *J. Mater. Chem. A* **2013**, *1*, 4610–4630; b) P. S. Goh, A. F. Ismail, S. M. Sanip, B. C. Ng, M. Aziz, *Sep. Purif. Technol.* **2011**, *81*, 243–264.

[4] a) J. T. Culp, L. Sui, A. Goodman, D. Luebke, *J. Colloid Interface Sci.* **2013**, *393*, 278–285; b) Z. Zhang, H. T. H. Nguyen, S. A. Miller, A. M. Ploskonka, J. B. DeCoste, S. M. Cohen, *J. Am. Chem. Soc.* **2016**, *138*, 920–925; c) T. Rodenas, I. Luz, G. Prieto, B. Seoane, H. Miro, A. Corma, F. Kapteijn, F. X. Llabrés Xamena, J. Gascon, *Nat. Mater.* **2015**, *14*, 48–55; d) W. Li, Y. Zhang, Q. Li, G. Zhang, *Chem. Eng. Sci.* **2015**, *135*, 232–257; e) B. Seoane, J. Coronas, I. Gascon, M. E. Benavides, O. Karvan, J. Caro, F. Kapteijn, J. Gascon, *Chem. Soc. Rev.* **2015**, *44*, 2421–2454; f) R. Adams, C. Carson, J. Ward, R. Tannenbaum, K. Koros, *Microporous Mesoporous Mater.* **2010**, *131*, 13–20; g) I. Erucar, G. Yilmaz, S. Keskin, *Chem. Asian J.* **2013**, *8*, 1692–1704; h) L. Zhang, Z. Hu, J. Jiang, *J. Phys. Chem. C* **2012**, *116*, 19268–19277; i) B. Zornoza, C. Tellez, J. Coronas, J. Gascon, F. Kapteijn, *Microporous Mesoporous Mater.* **2013**, *166*, 67–78.

[5] a) S. Shahida, K. Nijmeijera, S. Nehacheb, I. Vankelecomc, A. Deratanib, D. Quemener, *J. Membr. Sci.* **2015**, *492*, 21–32; b) J. Gascon, F. Kapteijn, B. Zornoza, V. Sebastia'n, C. Casado, J. Coronas, *Chem. Mater.* **2012**, *24*, 2829–2844; c) H. Vinh-Thang, S. Kaliaguine, *Chem. Rev.* **2013**, *113*, 4980–5028.

[6] a) R. Lin, L. Ge, L. Hou, E. Strounina, V. Rudolph, Z. Zhu, *ACS Appl. Mater. Interfaces* **2014**, *6*, 5609–5618; b) M. S. Denny, Jr., S. M. Cohen, *Angew. Chem. Int. Ed.* **2015**, *54*, 9029–9032; *Angew. Chem.* **2015**, *127*, 9157–9160; c) N. Tien-Binh, H. Vinh-Thang, X. Y. Chen, D. Rodriguea, S. Kaliaguine, *J. Mater. Chem. A* **2015**, *3*, 15202–15213; d) E. Ahmadi Feijani, T. Tavasoli, H. Mahdavi, *Ind. Eng. Chem. Res.* **2015**, *54*, 12124–12134.

[7] K. A. McDonald, J. I. Feldblyum, K. Koh, A. G. Wong-Foy, A. J. Matzger, *Chem. Commun.* **2015**, *51*, 11994–11996.

[8] W. Zhang, Y. Hu, J. Ge, H. L. Jiang, S. H. Yu, *J. Am. Chem. Soc.* **2014**, *136*, 16978–16981.

[9] S. Brunauer, P. H. Emmett, E. Teller, *J. Am. Chem. Soc.* **1938**, *60*, 309–319.

[10] D. Y. Siberio-Pérez, A. G. Wong-Foy, O. M. Yaghi, A. J. Matzger, *Chem. Mater.* **2007**, *19*, 3681–3685.

[11] a) P. I. Ravikovitch, G. L. Haller, A. V. Neimark, *Adv. Colloid Interface Sci.* **1998**, *76–77*, 203–226; b) P. I. Ravikovitch, A. V. Neimark, *J. Phys. Chem. B* **2001**, *105*, 6817–6823.

[12] P. Guo, D. Dutta, A. G. Wong-Foy, D. W. Gidley, A. J. Matzger, *J. Am. Chem. Soc.* **2015**, *137*, 2651–2657.

[13] a) G. Seu, *Dyes Pigm.* **1995**, *29*, 227–240; b) J. F. Deye, T. A. Berger, A. G. Anderson, *Anal. Chem.* **1990**, *62*, 615–622.

[14] a) M. Liu, A. G. Wong-Foy, R. S. Vallery, W. E. Frieze, J. K. Schnobrich, D. W. Gidley, A. J. Matzger, *Adv. Mater.* **2010**, *22*, 1598–1601; b) L. D. Tran, J. I. Feldblyum, A. G. Wong-Foy, A. J. Matzger, *Langmuir* **2015**, *31*, 2211–2217.

[15] a) F. R. Mayo, *J. Am. Chem. Soc.* **1953**, *75*, 6133–6142; b) F. R. Mayo, *J. Am. Chem. Soc.* **1968**, *90*, 1289–1295; c) K. S. Khuong, W. H. Jones, W. A. Pryor, K. N. Houk, *J. Am. Chem. Soc.* **2005**, *127*, 1265–1277; d) Y. Sun, Y. Wu, L. Chen, Z. Fu, Y. Sh, *Polym. J.* **2009**, *41*, 954–960.

[16] a) R. R. Hiatt, P. D. Bartlett, *J. Am. Chem. Soc.* **1959**, *81*, 1149–1154; b) W. C. Buzanowski, J. D. Graham, D. B. Priddy, E. Shero, *Polymer* **1992**, *33*, 3055–3059; c) W. A. Pryor, L. D. Lasswell, *AdV. Free-Radical Chem.* **1975**, *5*, 27–99.

Received: July 17, 2016
Published online: August 23, 2016

